

## Wide-Band $2N$ -Port $S$ -Parameter Extraction from $N$ -Port Data

Brian Young

**Abstract**—A technique is presented for extracting the full  $2N \times 2N$  set of  $S$ -parameters for an  $N$ -conductor interconnect from five sets of  $N$ -port  $S$ -parameter measurements on three specially prepared samples. Bandwidth is improved over prior techniques using two samples. Experiments confirm the bandwidth enhancement and illustrate the operational mechanism and accuracy expectations.

### I. INTRODUCTION

Packages for digital applications are typically characterized from either the outside (printed circuit board) or the inside (chip) to avoid practical difficulties with probing, including ports on opposite sides of the substrate, fine pitches, irregular grounds, molding, and lids [1]–[7]. A lumped model of an  $N$ -conductor interconnect can be constructed from measurements of two specially prepared samples [6], [7]: a short-circuited sample for resistance and inductance and an open-circuited sample for conductance and capacitance.

The lumped model represents a full  $2N$ -port model from which a  $2N \times 2N$   $S$ -parameter matrix can be derived. However, the  $2N \times 2N$   $S$ -parameter matrix is band-limited by the lumped approximation. An additional measurement on a third sample is introduced to enable the bandwidth of the data to be extended.

### II. THEORY

An  $N$ -conductor interconnect has a total of  $2N$  terminals. The goal is determine the  $2N \times 2N$   $S$ -parameters over a wide bandwidth from measurements performed on just  $N$  terminals on one side of the interconnect. The  $2N \times 2N$   $S$ -parameters can be subdivided into four  $N \times N$  blocks as

$$\begin{bmatrix} \bar{b}_1 \\ \bar{b}_2 \end{bmatrix} = \begin{bmatrix} \bar{\bar{S}}_A & \bar{\bar{S}}_B \\ \bar{\bar{S}}_C & \bar{\bar{S}}_D \end{bmatrix} \begin{bmatrix} \bar{a}_1 \\ \bar{a}_2 \end{bmatrix} \quad (1)$$

where, from reciprocity,  $\bar{\bar{S}}_C = \bar{\bar{S}}_B^T$ , where the subscript “1” indicates one side of the interconnect and “2” indicates the other.

Equation (1) can be specialized for three special termination cases to solve for the submatrices. For the first sample, assume that ports  $N+1$  to  $2N$  are shorted to ground, then  $\bar{b}_2 = -\bar{a}_2$  and (1) reduces to  $\bar{b}_1 = [\bar{\bar{S}}_A - \bar{\bar{S}}_B(\bar{I} + \bar{\bar{S}}_D)^{-1}\bar{\bar{S}}_C]\bar{a}_1$  so the  $N \times N$   $S$ -parameter matrix measured at ports 1 to  $N$  can be defined as

$$\bar{\bar{S}}_s = \bar{\bar{S}}_A - \bar{\bar{S}}_B(\bar{I} + \bar{\bar{S}}_D)^{-1}\bar{\bar{S}}_C. \quad (2)$$

Similarly, for the second sample with ports  $N+1$  to  $2N$  open, then

$$\bar{\bar{S}}_o = \bar{\bar{S}}_A + \bar{\bar{S}}_B(\bar{I} - \bar{\bar{S}}_D)^{-1}\bar{\bar{S}}_C. \quad (3)$$

Finally, for the third sample with ports  $N+1$  to  $2N$  matched, then

$$\bar{\bar{S}}_m = \bar{\bar{S}}_A. \quad (4)$$

Manuscript received September 15, 1997; revised May 6, 1998.

The author is with Motorola, Austin, TX 78730 USA.

Publisher Item Identifier S 0018-9480(98)06152-3.

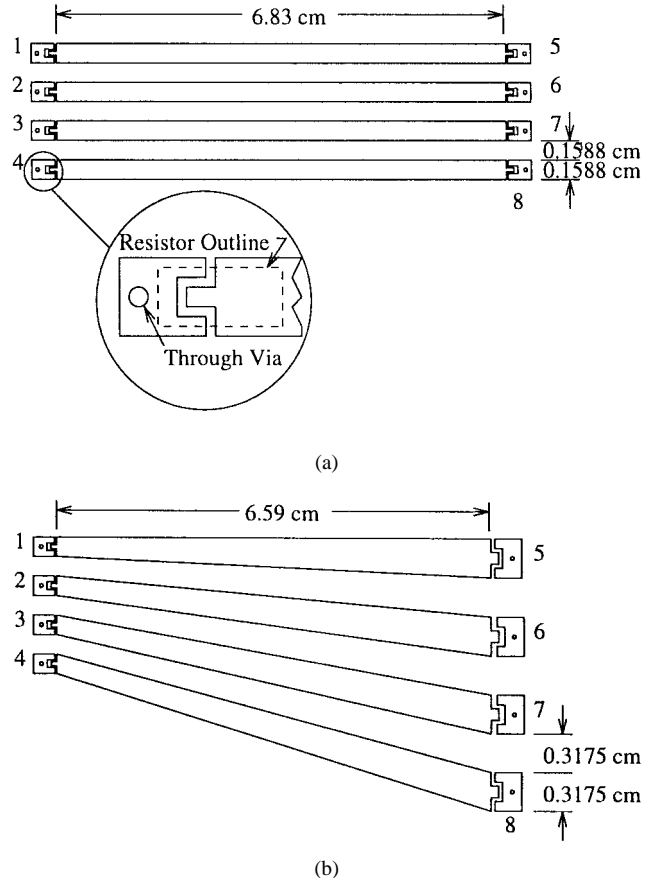


Fig. 1. Layouts for the four-conductor sample interconnects. (a) Parallel straight lines. (b) Nonparallel tapered lines.

Eliminating  $\bar{\bar{S}}_A$  and  $\bar{\bar{S}}_D$  from (2)–(4) yields the quadratic equation

$$\bar{\bar{S}}_B \bar{\bar{S}}_B^T = 2[(\bar{\bar{S}}_o - \bar{\bar{S}}_m)^{-1} - (\bar{\bar{S}}_s - \bar{\bar{S}}_m)^{-1}]. \quad (5)$$

Assuming  $\bar{\bar{S}}_B$  has been found, the remaining submatrices of (1) are then given by (4) and

$$\bar{\bar{S}}_D = -\frac{1}{2}\bar{\bar{S}}_C[(\bar{\bar{S}}_s - \bar{\bar{S}}_m)^{-1} + (\bar{\bar{S}}_o - \bar{\bar{S}}_m)^{-1}]\bar{\bar{S}}_B. \quad (6)$$

Since  $\bar{\bar{S}}_C = \bar{\bar{S}}_B^T$ , any sign information contained in  $\bar{\bar{S}}_B$  is lost as (6) is multiplied out. The sign of  $\bar{\bar{S}}_D$  can be recovered by comparison to the initial guess.

Equation (5) is of the generic form  $\bar{\bar{A}}\bar{\bar{A}}^T = \bar{\bar{B}}$ , where  $\bar{\bar{B}}$  is known and  $\bar{\bar{A}}$  is to be found. Each solution can be found as a zero of the function  $\bar{F} = \bar{\bar{A}}^T - \bar{\bar{A}}^{-1}\bar{\bar{B}}$ , which can be solved using the standard Newton–Raphson methodology. The Jacobian can be found analytically, and the basic derivative needed is

$$\frac{\partial \bar{F}}{\partial A_{ij}} = \frac{\partial \bar{\bar{A}}^T}{\partial A_{ij}} + \bar{\bar{A}}^{-1} \frac{\partial \bar{\bar{A}}}{\partial A_{ij}} \bar{\bar{A}}^{-1} \bar{\bar{B}}$$

where

$$\frac{\partial \bar{\bar{A}}}{\partial A_{ij}} = \begin{cases} 0, & m \neq i, n \neq j \\ 1, & m = 1, n = j. \end{cases}$$

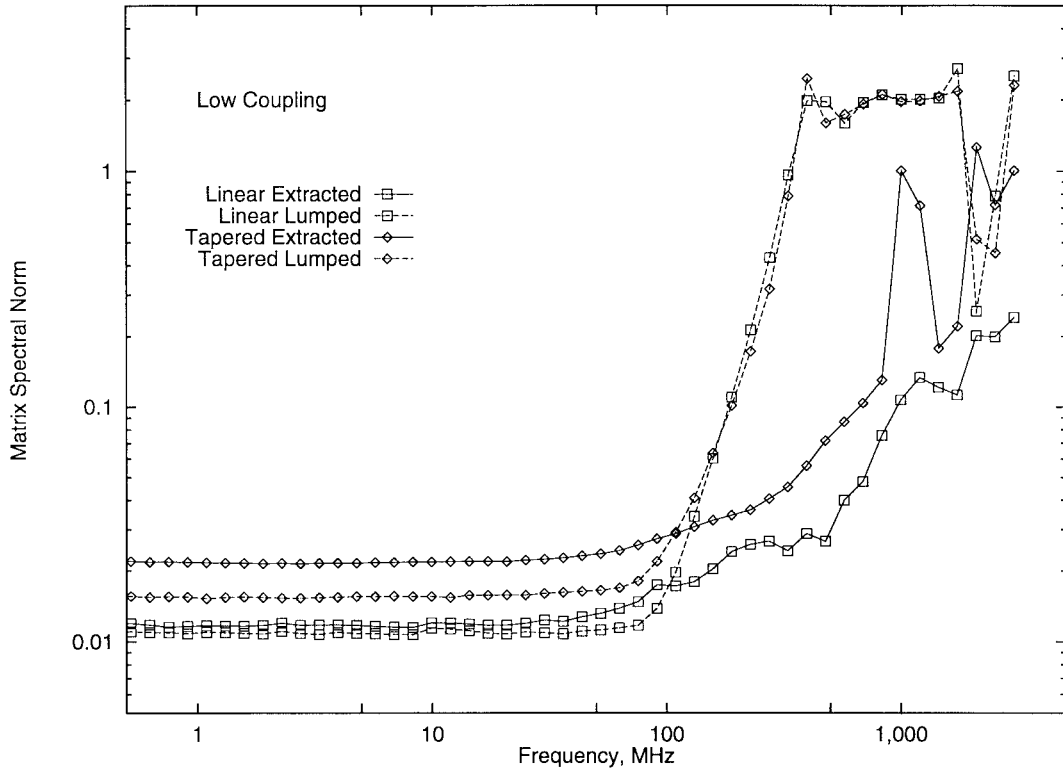


Fig. 2. Error plot comparing the extracted and lumped models to the full measurement for the low-coupling cases.

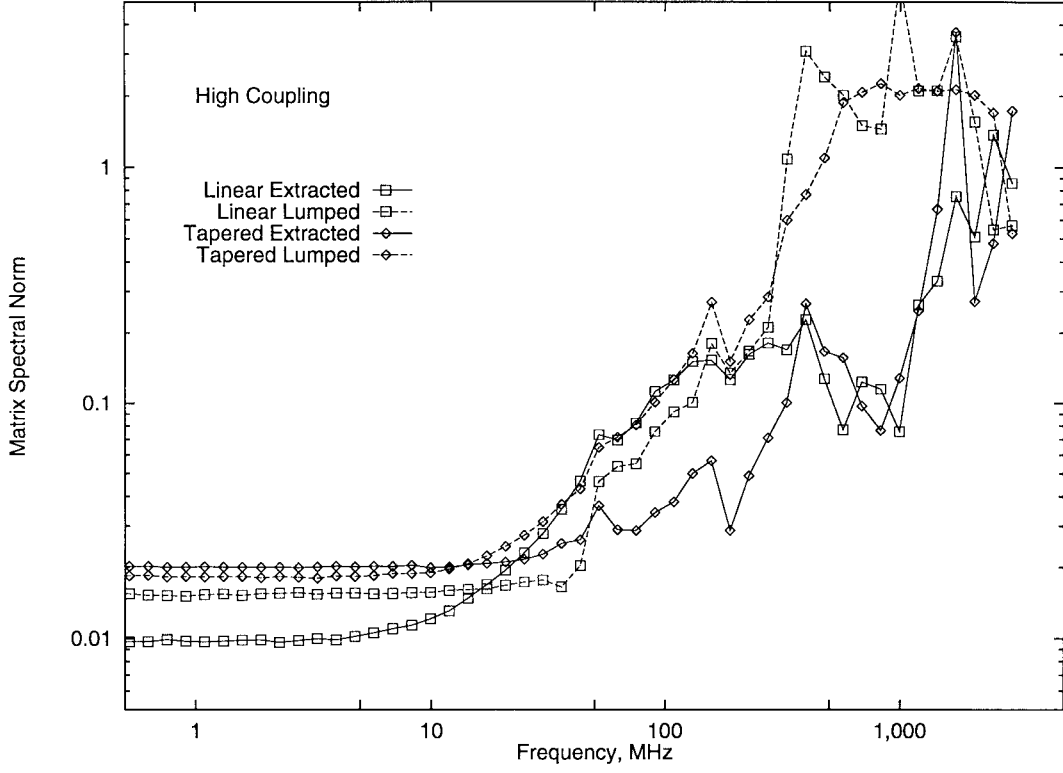


Fig. 3. Error plot comparing the extracted and lumped models to the full measurement for the high-coupling cases.

The initial guess at a given frequency is provided by the solution from the next lower frequency. By starting low and sweeping up in frequency, the strategy enables the extraction of wide bandwidth.

To find the initial guess at the lowest frequency, measurements on the shorted and opened sample (using the technique in [7]) result

in the  $N \times N$  impedance matrices  $\bar{Z}_s$  and  $\bar{Z}_o$ , respectively. The  $2N \times 2N$  impedance matrix is then

$$\bar{Z} = \begin{bmatrix} \frac{1}{2}\bar{Z}_s + \bar{Z}_o^{-1} & \bar{Z}_o^{-1} \\ \bar{Z}_o^{-1} & \frac{1}{2}\bar{Z}_s + \bar{Z}_o^{-1} \end{bmatrix}. \quad (7)$$

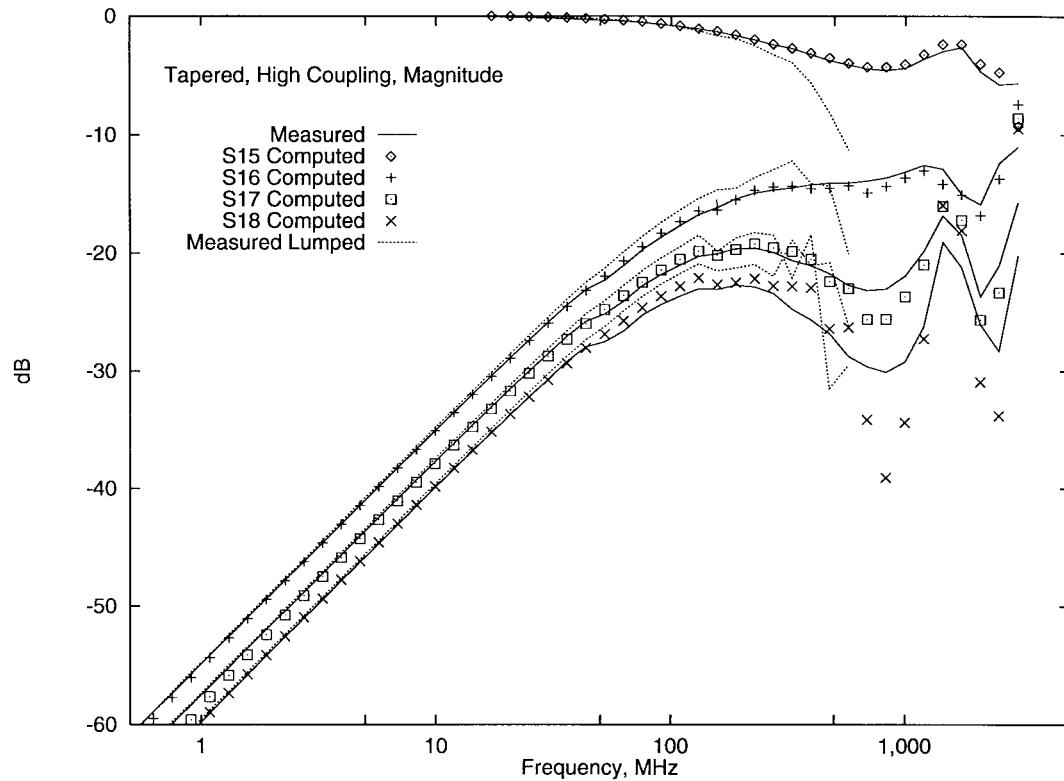


Fig. 4.  $S$ -parameter magnitude plots for  $S_{15}$  to  $S_{18}$ , comparing the extracted and lumped models to the full measurement for the tapered lines with high coupling.

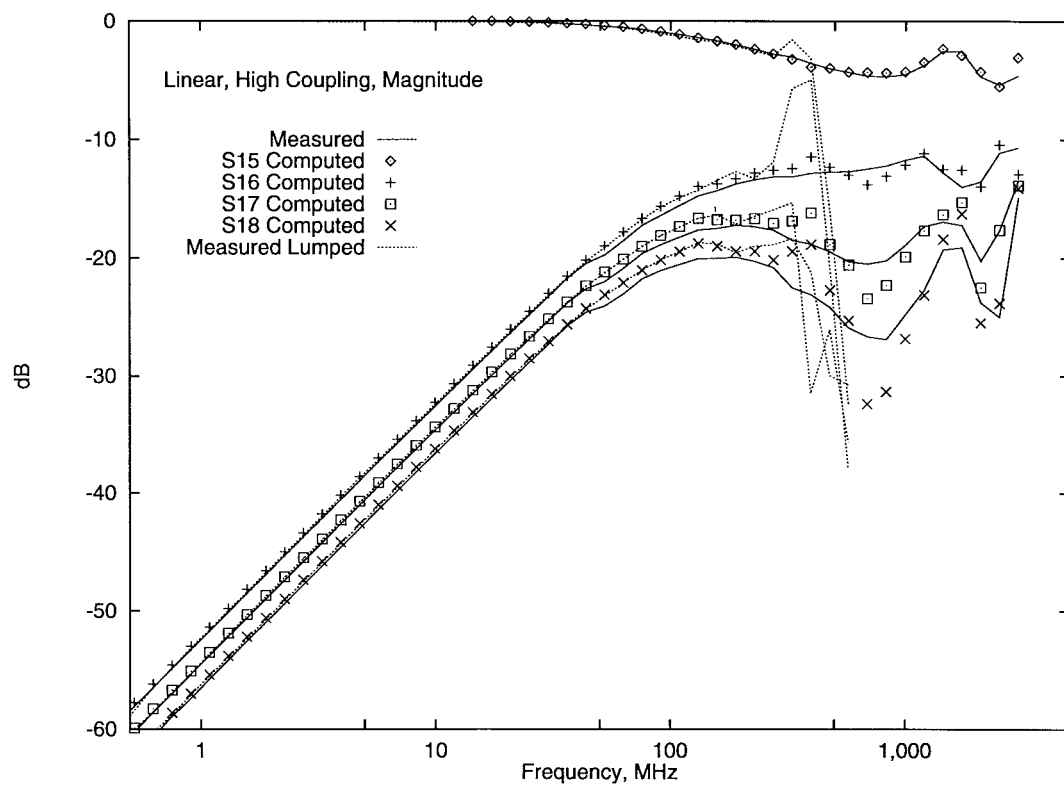


Fig. 5.  $S$ -parameter magnitude plots for  $S_{15}$  to  $S_{18}$ , comparing the extracted and lumped models to the full measurement for the straight lines with high coupling.

The  $2N \times 2N$   $S$ -parameter matrix is computed as  $\bar{\bar{S}} = (\bar{\bar{Z}} + Z_o \bar{\bar{I}})^{-1} (\bar{\bar{Z}} - Z_o \bar{\bar{I}})$ , where  $Z_o$  is the characteristic impedance.

### III. MEASUREMENTS

The two patterns in Fig. 1 are characterized with two different gaps to the ground plane: 0.8 mm with FR-4 dielectric, and 1 cm with air plus a thin FR-4 support. The two patterns and spacings combine to cover the following four cases:

- 1) symmetry with low coupling;
- 2) symmetry with high coupling;
- 3) asymmetry with low coupling;
- 4) asymmetry with high coupling.

All measurements are performed with a two-port vector network analyzer using microwave coaxial probes. Matched terminations are  $50.4\Omega$  surface-mount chip resistors hand soldered onto the probe pads, as shown schematically in Fig. 1(a).

For each of the four interconnects, six sets of multiport data are collected. Five sets of  $4 \times 4$  matrices are collected at ports 1–4 and used to extract the full  $8 \times 8$   $S$ -parameter matrix using the technique detailed above. One  $8 \times 8$   $S$ -parameter matrix is measured at ports 1–8. To establish a reference on bandwidth expansion, the  $8 \times 8$   $S$ -parameter matrix derived from (7) is also computed and referred to as the “lumped model.”

### IV. RESULTS AND DISCUSSION

The extracted  $8 \times 8$  result is compared to the full measurement by computing the spectral norm of the error matrix  $\bar{e} = \bar{\bar{I}} - \bar{\bar{S}}_{\text{extracted}}^{-1} \bar{\bar{S}}_{\text{measured}}$ , where the spectral norm is given by the magnitude of the largest eigenvalue. The error is similarly defined for the lumped model.

For the low-coupling case, the results in Fig. 2 show that the extracted data inflects at the same 100-MHz frequency as the lumped model, but onto a different slope. Selecting 0.1 as the upper limit on the error matrix norm, then the extracted  $S$ -parameters, achieve a  $3.6\times$  improvement in bandwidth.

For the high-coupling case, shown in Fig. 3, a mixture of behavior is observable. The tapered lines behave as in Fig. 2 with an inflection point of 50 MHz, and the bandwidth improvement at an error matrix norm of 0.1 is, again,  $3.6\times$  the lumped model. The linear lines track with the lumped model until about 200 MHz before breaking to a lower level of error. The extraction method provides no bandwidth improvement for the linear lines unless the limit on the error matrix norm is relaxed to 0.3, where the bandwidth improvement is  $4.7\times$ .

Two modes of extraction are at work. The swept magnitude plot in Fig. 4 shows representative data for all cases, except the linear high-coupling case. The extracted  $S$ -parameters track the measured  $S$ -parameters at all frequencies until significant error is encountered at high frequencies. In contrast, the plot in Fig. 5 for the linear high-coupling case shows that the extracted  $S$ -parameters track the lumped  $S$ -parameters until the lumped approximation fails, then the extracted data jumps to track the measured  $S$ -parameters.

The swept plots in Figs. 4–5 also show that the utility of the data can be much greater than that implied by the norm of the error matrix. For the important  $S$ -parameters, i.e., for transmission on a line and coupling to neighbors, the extracted  $S$ -parameters are quite useful for frequencies up to the limit of the experiment.

### V. CONCLUSION

Lumped modeling enables probing of just one side of an interconnect by characterizing two samples, where the unprobed side is left either open or is shorted to ground. Impedance matrix measurements

of the two samples complete the model. In this paper, it is shown that a third sample, with the unprobed side terminated with matched loads, enables the bandwidth of the data to be extended using  $S$ -parameter matrix measurements of the three samples. The number of measurements required are the two  $Z$ -matrix measurements for the starting lumped model, plus three  $S$ -matrix measurements for bandwidth expansion.

Two distinct extraction behaviors are observed. The extracted data tracks either the full measurement at lower frequencies or the lumped model. For the four cases examined here, three track the full measurement while one tracks the lumped model. Numerical experimentation could not force the data to change tracks.

The accuracy of the extracted data depends on the limit set for the error matrix norm and on the extraction behavior. For the interconnects tested in this paper, bandwidth expansion is by approximately a factor of four. The bandwidth expansion can exceed  $10\times$  for the  $S$ -parameters of through connections and for coupling to near neighbors.

### REFERENCES

- [1] D. Carlton, K. Reed, K. Jones, and E. Strid, “Accurate measurement of high-speed package and interconnect parasitics,” in *IEEE/CHMT Japan IEMT Symp. Dig.*, 1989, pp. 276–279.
- [2] J. Williams, K. Smith, and E. Godshalk, “Improved techniques for characterization of high-speed packaging,” *Proc. Int. Symp. Microelectronics*, Oct. 1991, pp. 262–266.
- [3] C. Stanghan and B. MacDonald, “Electrical characterization of packages for high-speed integrated circuits,” *IEEE Trans. Comp., Hybrids, Manufact. Technol.*, vol. CHMT-8, pp. 468–473, Dec. 1985.
- [4] C.-T. Tsai and W.-Y. Yip, “An experimental technique for full package inductance matrix characterization,” *IEEE Trans. Comp., Packag., Manufact. Technol. B*, vol. 19, pp. 338–343, May 1996.
- [5] P. Harvey, A. Kinningham, and C. Schmolze, “Electrical characterization of a tape ball grid array package,” in *Proc. Int. Electron. Packaging Conf.*, 1995, pp. 775–786.
- [6] A. Agrawal, K.-M. Lee, L. Scott, and H. Fowles, “Experimental characterization of multiconductor transmission lines in the frequency domain,” *IEEE Trans. Electromag. Compat.*, vol. EMC-21, pp. 20–27, Feb. 1979.
- [7] B. Young and A. Sparkman, “Measurement of package inductance and capacitance matrices,” *IEEE Trans. Comp., Packag., Manufact. Technol. B*, vol. 19, pp. 225–229, Feb. 1996.